

Research Article

Numerical Study of a Self Priming Regenerative Pump for Improved Performance using Geometric Modifications

K. Vasudeva Karanth[†], Manjunath M. S.[†], Shiva Kumar[†] and N. Yagnesh Sharma^{**}

[†]Department of Mechanical & Mfg. Engineering, Manipal Institute of Technology, Manipal University, India

Accepted 09 Jan 2015, Available online 01 Feb 2015, Vol.5, No.1 (Feb 2015)

Abstract

Regenerative centrifugal pumps (RCP) have gained significance in industry as these pumps produce less noise and have low specific speed. They are compact in size but capable of delivering high heads with stable performance characteristics. Regenerative pumps are classified as turbo machines that can develop high static head within a single stage. In this paper, the use of Computational Fluid Dynamics (CFD) for simulating and analyzing the flow field within a regenerative pump and validation study of the CFD results with the experimental work is presented. Several numerical models were analyzed in the study for performance enhancement. It is observed that for configurations having greater number of impeller vanes, static pressure developed by the pump, increased significantly and vice versa. For configurations with splitter vanes introduced near the vicinity of the outlet chamber of the pump, the performance of the pump increased to a greater extent due to reduction in the large recirculation zone which occurs near the exit flow path. Also the configuration having radial inlet and exit chamber with constant width showed a significant improvement in the performance when compared to the base model.

Keywords: Regenerative pump, Rotating stall, Unsteady Analysis, splitter vanes, In-mold, Time periodic.

1. Introduction

Regenerative centrifugal pumps (RCP) have the unique characteristics of producing less noise and have low specific speeds. They are compact and are capable of developing high heads with stable performance characteristics. Because of these features they are gaining significance these days for industrial and domestic applications. According to John (1953) the regenerative pump has excited inventors, engineers and manufacturers due to its unique design and operational characteristics. Fundamentally a regenerative pump is a hydro-dynamic machine that follows the same laws of similitude that are applicable to axial flow, mixed flow and centrifugal flow turbo machines. It is observed that there is a considerable total manometric head developed by this pump even for relatively low mass flow rates. As this machine comes under the class of turbomachines it becomes quite suitable for large industrial applications.

According to Mueller (2004), a regenerative pump is a turbo-machine which produces high kinetic energy like that of radial flow centrifugal pumps. However these pumps can be used as a better and efficient alternative in most of the applications. The pump has a

construction in which the fluid enters a set of radial impeller teeth which guides the fluid from the inlet to the outlet, both separated by a 320° annulus chamber producing a toroidal motion also known as regenerative flow according to Hopkins (1953).

The complex flow-field within the pump represents a significant challenge for detailed analytical modeling, as described by Badami (1997) and Engeda (2003). Song *et al.* (2003) developed an improved and modified theoretical model that can explain the change in the circulatory flow caused by variation in channel area. Several loss models were assumed by the authors and the results of predictions were compared with experimental and CFD data. Meakhaail and Park (2005) improved the performance of a regenerative pump by adopting an improvised model. The model had two exit angles for the impeller blades with one inlet angle which showed an improvement in the pump head and efficiency.

The new model showed that the side-blade exit angle contributed to the performance of regenerative pump, unlike the earlier theory. Fransis *et al.* (2011) carried out experimental and numerical analysis to simulate the flow field inside a regenerative pump and validate its performance. Won *et al.* (2013) found that blade geometry and the blade angles contributed significantly for the efficiency and pressure head developed by the regenerative pump. Among all blade configurations, the highest head with reasonably good

*Corresponding author: N. Yagnesh Sharma, Department of Mechanical and Manufacturing Engineering, Manipal Institute of Technology, Manipal University, Manipal 576104 India.

efficiency was obtained by adopting Chevron blade. Also it was observed that the best performance for Chevron blade angle was at around 30° , after comparison.

The above literature indicates that the effect of varying the number of impeller vanes and the effect of making geometrical changes on the inlet, outlet and side flow passage of the pump on its performance have not been the focus of study and hence an attempt has been made to numerically establish the effect of the above geometrical modification on the performance parameters of the pump.

The impeller of regenerative pump used in the study is shown in figure 1. The performance parameters of the pump were recorded before the pump was dismantled for geometrical measurement. Using the measured geometric details the numerical model was constructed and the CFD analysis was carried out. The numerical model was then validated with experimental results. Figure 2 shows the pictorial view of the dismantled impeller.

2. Numerical Modeling

2.1 Geometry and Mesh Generation

The numerical model of the pump consists of an inlet region with 144000 elements, an impeller with 36×2 impeller vane fluid continuums of 6000 elements each, a 3000 element annular region outside the impeller which is integral with fluid continuum on either sides of the impeller, altogether containing 1,538,592 elements. An outlet passage containing 144,000 elements. The number of elements in the whole of fluid domain consists of 2,258,593 hexahedral elements.

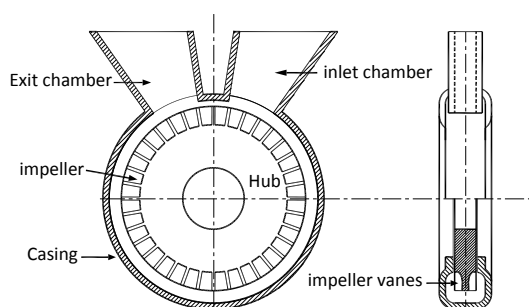


Fig.1 Sectional view of the pump



Fig. 2 Pictorial view of the pump impeller

For establishing grid independency, analysis was carried out with number of elements limited to approximately 1.5 million, 1.8 million, 2.3 million, 2.7 million and 3.2 million elements. Since the variation in the pressure values was not more than 0.5% for configurations containing elements that are greater than 2.3 million, configuration with 2.3 million was adopted to save the computational time. Figure 3 shows the localized view of the meshed configuration adopted in the numerical study.

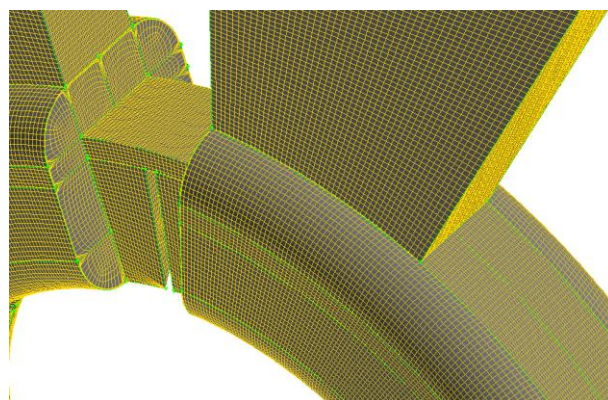


Fig. 3 Localized view of the meshed domain

2.2 Unsteady Formulation

Three dimensional unsteady RANS equations set to polar co-ordinate system are used in the CFD analysis and the Fluent code (2012) is adopted. The boundary conditions used are, 'mass flow inlet' at the entry of the pump and at the outlet flange of the pump, pressure outlet condition set to atmospheric pressure is applied. For the casing and the vanes, a zero slip wall condition is specified along the flow path. Since the flow is highly turbulent the flow behavior is simulated using a standard $k-\epsilon$ model. The turbulent intensity is limited to 5%. The turbulent length scale which is approximately cube root of the pump volume is calculated to be equal to 0.0278 m and is adopted in the analysis. The solver is pressure based and the unsteady formulation used is a second order implicit velocity formulation. Discretization is carried out with the help of second order upwind scheme. SIMPLE algorithm is adopted for coupling the pressure and velocity.

Sliding mesh formulation is used to simulate the rotating impeller of the pump and the mesh interface zones are applied at the interfaces between the stationary fluid domain and the rotating impeller domain. The relative position between the rotating impeller mesh and the stationary fluid mesh is changed with every time step. The time step Δt is set to 5.78704×10^{-5} seconds, which is the time for 1° rotation of the impeller for a rated speed of 2880 rpm. Every time step is carried for a maximum of 30 iterations and the convergence criterion for x, y, z velocities, continuity equation, k and epsilon for turbulence are limited to 1×10^{-6} . The flow parameters such as velocity

and pressure are monitored at prominent locations of the flow domain such as outlet and inlet of the pump and the unsteady analysis is carried out until the pressure fluctuations measured at these salient locations have become time periodic in nature. It is observed in this study that the pressure fluctuations have reached a time periodic state after three rotations of the impeller and hence the flow parameters for calculating the performance parameters are recorded after three rotations of the impeller.

At each prominent zone in the computational domain, the area weighted average values of the static and total pressure and velocity, corresponding to each time step is recorded. A time weighted average value of these parameters is then calculated over the time steps, for the purpose of comparison of various configurations.

3. Validations of Numerical Results

The numerical work in this study is calibrated with the experimental results for the purpose of validation of numerical results. Fig. 4 presents the validation graph for the numerical results with the experimental results. In this graph it can be noted that the head coefficient ψ decreases with increase in flow coefficient ϕ , as is required for a regenerative pump. The terms flow coefficient ϕ and pressure coefficient ψ are calculated using equations (a) and (b) respectively as defined by Francis *et. al.* (2011).

$$\phi = \frac{\dot{m}}{\omega D^2} \text{ --- (a) } \psi = \frac{gh}{\omega^2 D^2} \text{ --- (b)}$$

It can be observed from the graph shown in figure 4 that the experimental results and numerical results are very close to each other.

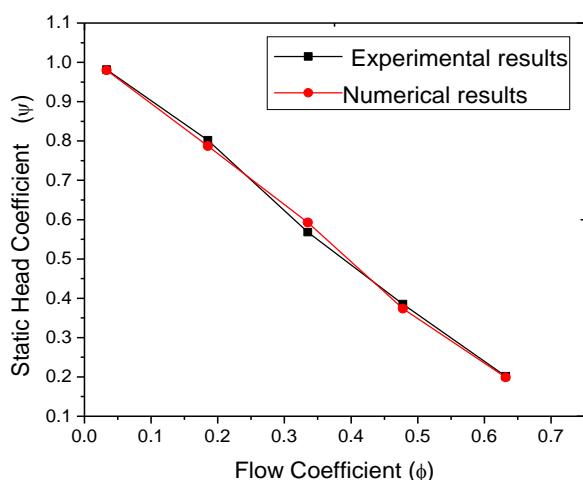


Fig. 4 Head coefficient vs Flow coefficient Validation graph

4. Configurations with Geometric Modifications

Five numerical configurations are adopted in the study. Configuration 1 is the regenerative pump with 36 impeller vanes which is the model for which validation

is carried out as shown in figure 1. Configuration 2 has 32 impeller vanes as presented in figure 5. Figure 6 shows configuration 3 which has 40 impeller vanes.

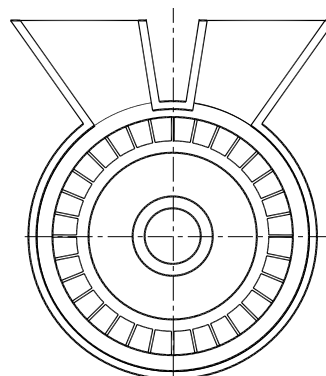


Fig -5: Configuration 2 which has 32 impeller vanes

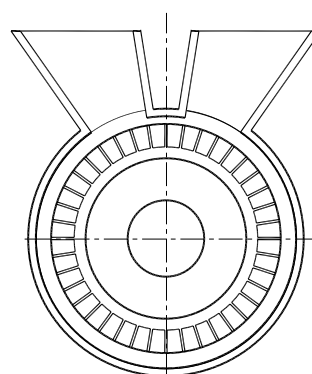


Fig. 6 Configuration 3 which has 40 impeller vanes

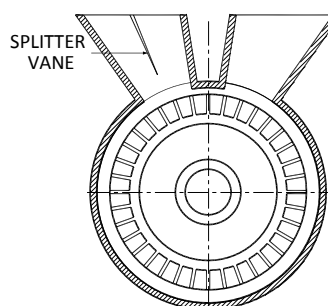


Fig. 7 Configuration 4 which has splitter vanes across the exit chamber

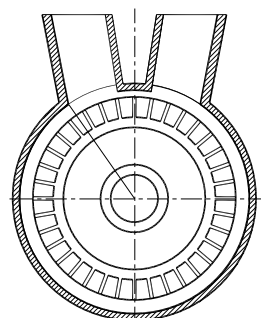


Fig. 8 Configuration 5 which has radial inlet and exit chamber with constant width

Configuration 4 has splitter vanes introduced across the exit chamber (figure 7). Configuration 5 has radial passage with constant width for inlet and exit chambers as presented in figure 8.

5. Results and Discussion

The numerical analysis is carried out corresponding to the design point mass flow rate and this mass flow rate is determined from the experimental study of the regenerative pump. The static pressure rise coefficient ψ_s and total pressure rise coefficient ψ_T for the five configurations are recorded and compared after the unsteady analysis has reached a time periodic state. Here, $\psi_s = g\Delta h_{static} / \omega^2 D^2$, $\psi_T = g\Delta h_{Total} / \omega^2 D^2$ Where, Δh represents the net pressure rise across the pump.

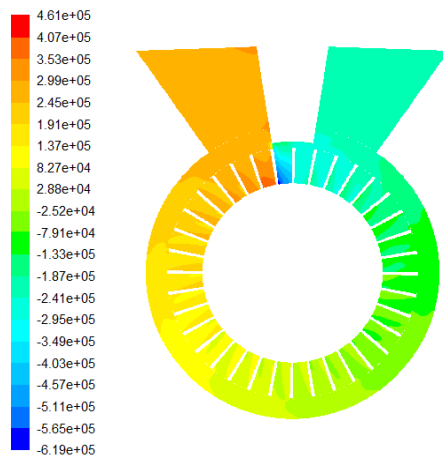


Fig. 9(a) Pressure contour plot for configuration 1

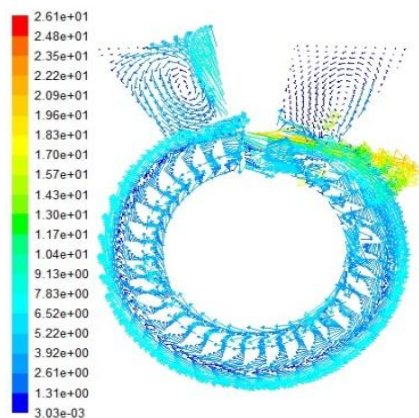


Fig. 9(b) Velocity vector plot for configuration 1

Figure 9(a) shows the contour plot for static pressure distribution across the pump for configuration 1 captured on a vertical plane which is at an axial distance of 3.4 mm from the central plane.

Figure 9(b) shows the velocity vector plot for configuration 1 where a large recirculation zone is observed in the exit chamber of the pump. This recirculation leading to a rotating stall can be attributed to the reasoning that the fluid takes an

abrupt turn towards the exit chamber from the passage of the impeller leading to a rotational movement before it moves towards the exit flange of the pump. A toroidal motion of the fluid is also clearly observed around the impeller which is causing the pressure compounding taking place from one impeller vane to the next, as the fluid moves towards the exit chamber.

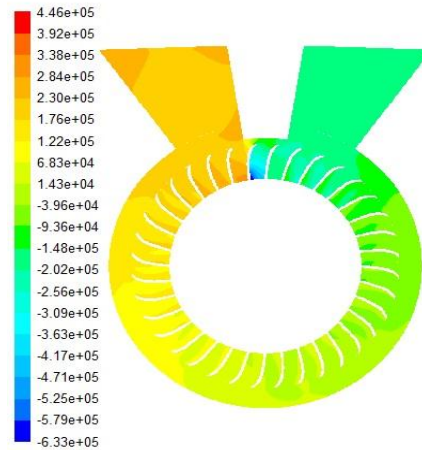


Fig. 10(a) Pressure contour plot for configuration 2

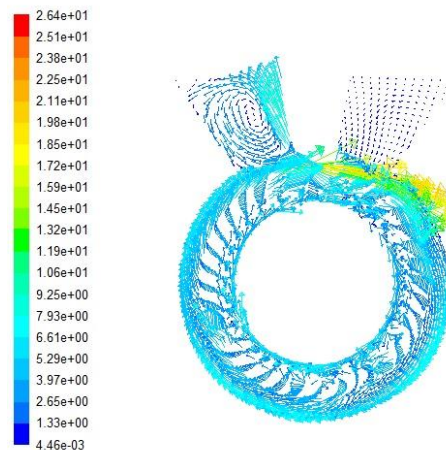


Fig. 10(b) Velocity vector plot for configuration 2

Figures 10(a) and 10(b) show the contour plot and velocity vector plot for configuration 2 which has 32 impeller vanes. The static pressure rise across the pump is 13.3% lower than that of configuration 1 (which has 36 impeller vanes) as can be seen in figure 14. The total pressure is lower by 25% for the same configuration, as can be noted in figures 15 and 16. This can be attributed to the fact that there are lesser number of pressure compounding stages of the impeller due to the presence of only 32 impeller vanes compared to 36 vanes for configuration 1. It can also be noted from figures 14 and 15 that the static and total pressure coefficients at the suction and delivery sides are lower compared to that of configuration 1. Figures 11(a) and 11(b) show the static pressure contour plot and vector plots for configuration 3 which has 40 vanes. It can be noted from figures 16 that the increase

in the number of vanes from 36 to 40 results in a remarkable increase in static pressure coefficient by 13.8% whereas the total pressure rise is only 4% compared to that of configuration 1. The significant static pressure rise is due to pressure compounding effect as can be observed from figure 10(a). However the smaller percentage rise in total pressure can be attributed to the reasoning that the fluid loses its kinetic head with more number of vanes for the same rotational speed.

Figures 12(a) and 12(b) show the static pressure contour plot and velocity vector plot for configuration 4 which has a splitter vane introduced across the exit chamber. It is observed from the velocity vector plot that the rotating stall that exists for configuration 1 in the flow passage of the exit chamber is reduced significantly and hence contributing to 1% rise in static pressure and 4.6% rise in total pressure across the pump.

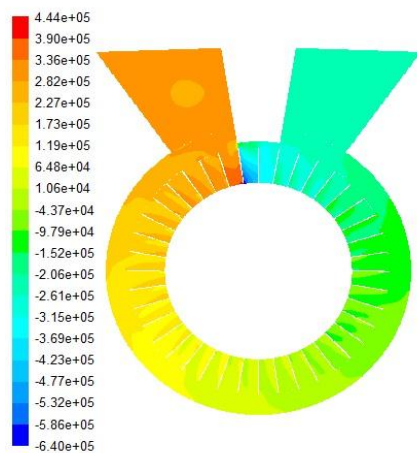


Fig. 11(a) Pressure contour plot for configuration 3

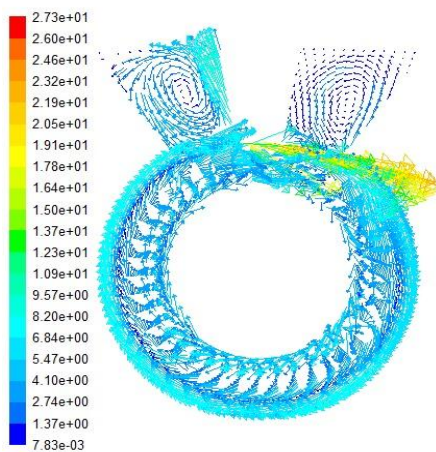


Fig. 11(b) Velocity vector plot for configuration 3

For configuration 5 which has a radial inlet and exit chamber with constant width, the static pressure rise across the pump is 1.8% and the total pressure rise across the pump is 2.9% compared to that of configuration 1. The improvement in the pressure,

across the pump can be attributed to the fact that there is a reduction in the large rotating stall that exits at the inlet and exit chamber as can be observed in fig. 13(b) compared to that of the base model configuration 1. Figure 13(a) shows the pressure contour plots for configuration 5 which shows a wider range of pressure contours compared to figure 9(a).

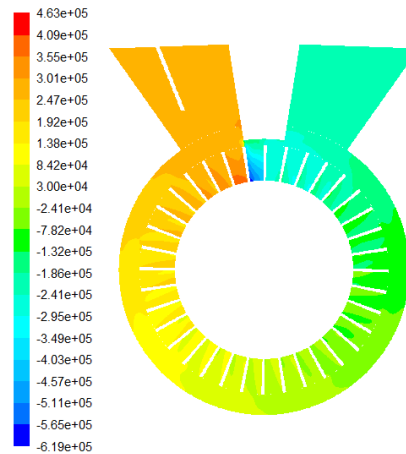


Fig. 12(a) Pressure contour plot for configuration 4

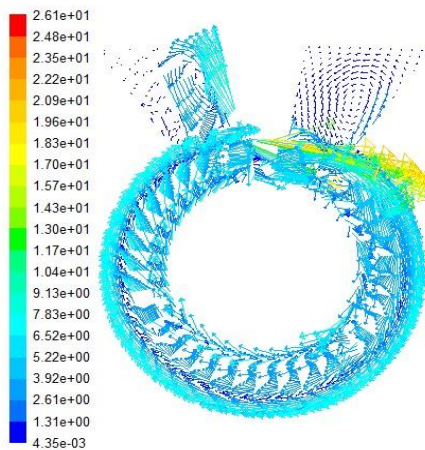


Fig. 12(b) Velocity vector plot for configuration 4

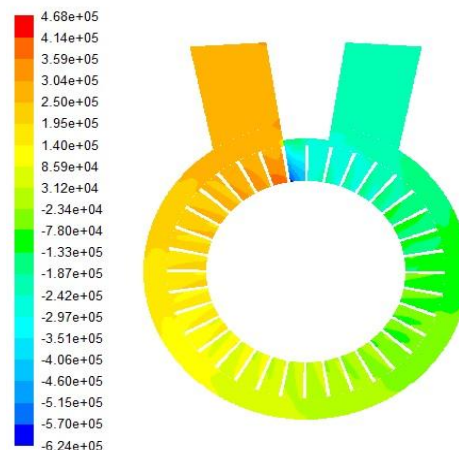


Fig. 13(a) Pressure contour plot for configuration 5

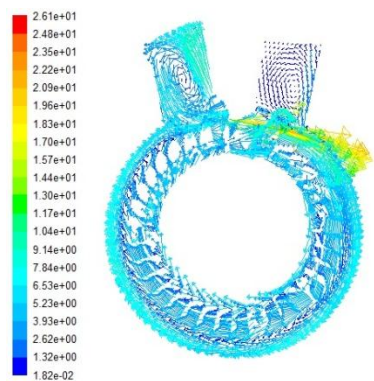


Fig. 13(b) Velocity vector plot for configuration 5

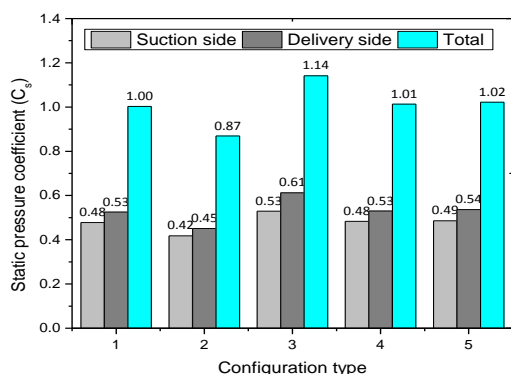


Fig. 14 Comparative bar diagrams for static pressure rise coefficient

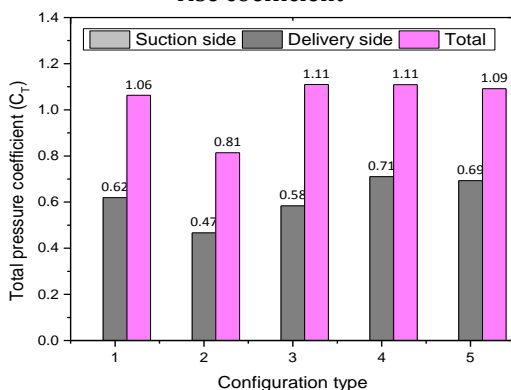


Fig. 15 Comparative bar diagrams for total pressure rise coefficient

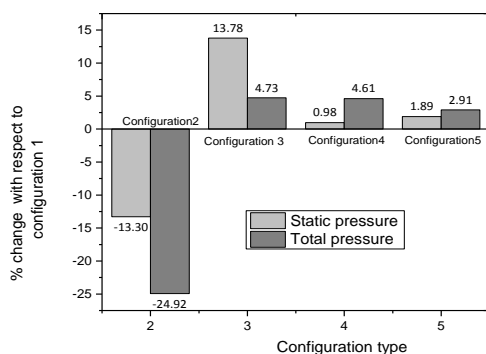


Fig. 16 Comparative bar diagrams for percentage change in static and total pressure rise across the pump

Conclusions

The numerical study using computational fluid dynamics as a tool helps in visualizing the complex flow phenomena that exists in a regenerative pump and the following conclusions are drawn from the study.

- 1) The number of impeller vanes will contribute significantly in terms of static pressure rise across the pump as more number of impeller vanes will help in the pressure compounding phenomena.
- 2) Introducing a splitter vane at the exit chamber will facilitate in reducing the rotating stall and thereby leading to improved static and total pressure rise across the pump.
- 3) Modification of Inlet and exit chamber geometry with a radial passage of constant width helps in reducing the large rotating stall and hence contributing to the static pressure rise across the pump

Acknowledgement

The computational facilities and finance were extended by the Department of Mechanical and Manufacturing Engineering, Manipal Institute of Technology, Manipal University, India, which is thankfully acknowledged.

References

Badami M, (1997), Theoretical and experimental analysis of traditional and new periphery pumps. *SAE Technical Papers Series*, No 971074, DOI:10.4271/971074

Engeda A. (2003) Flow analysis and design suggestions for regenerative flow pumps *ASME FEDSM2003-45681*

Fluent 14, (2011), Ansys Inc., Cavendish Court Lebanon, NH, 03766, USA

Francis Quail, Thomas Scanlon, Matthew Stickland, (2011) Design optimization of a regenerative pump using numerical and experimental techniques, *International Journal of Numerical Methods for Heat & Fluid Flow*, Volume 21, Issue 1, pp 95 - 111,

Hopkins T.J., (1953), Theoretical and experimental analysis of a regenerative pump, *Research report*, Massachusetts Institute of Technology, 1953.

John Albert Oerich, (1953) Development of an analysis of a regenerative pump Research, report, Massachusetts Institute of Technology, 1953.

Meakhail T. and Park S. O., (2005), An improved theory for regenerative pump performance, *Proceedings of the Institution of Mechanical Engineers, Part A: Journal of Power and Energy*, Vol. 219, pp. 213 - 222.

Mueller, S. (2004), Consider regenerative pumps for low flow/low NPSH applications. *Hydrocarbon processing* Aug. 2004 report, pp. 55-57.

Song J. W., Engeda A., Chung M. K. (2003), A modified theory for the flow mechanism in a regenerative flow pump, *Proceedings of the Institution of Mechanical Engineers, Part A: Journal of Power and Energy*, Vol. 217, pp. 311 - 321.

Won C. C., Il Su Yoo, Park M. R. and Myung K. C., (2013), Experimental study on the effect of blade angle on regenerative pump performance, *Proceedings of the Institution of Mechanical Engineers, Part A: Journal of Power and Energy* DOI: 10.1177/0957650913487731